Silibinin Inhibits Colorectal Cancer Growth by Inhibiting Tumor Cell Proliferation and Angiogenesis

Rana P. Singh,[1,3] Mallikarjuna Gu,[1] and Rajesh Agarwal[1,2]

[1]Department of Pharmaceutical Sciences, School of Pharmacy and [2]University of Colorado Cancer Center, University of Colorado Denver, Denver, Colorado and [3]Cancer Biology Laboratory, School of Life Sciences, Jawaharlal Nehru University, New Delhi, India

Abstract

Herein, for the first time, we investigated *in vivo* efficacy and associated molecular biomarkers and mechanisms of a chemopreventive agent, silibinin, against human colorectal carcinoma (CRC) HT29 xenograft growth. Nude mice were implanted with HT29 cells and fed with vehicle (carboxymethyl cellulose or phosphatidylcholine) or 200 mg/kg/d dose of silibinin or 100 and 200 mg/kg/d doses of silybin-phytosome (5 days per week) for 32 days. Silibinin inhibited tumor growth that accounted for 48% ($P = 0.002$) decrease in tumor volume and 42% ($P = 0.012$) decrease in tumor weight at the end of the experiment without any adverse health effect. A stronger antitumor efficacy was observed with silybin-phytosome preparation. Silibinin decreased proliferation index by 40% ($P < 0.001$), increased apoptotic index by ~2-fold ($P = 0.001$), and reduced microvessel density by 36% ($P = 0.001$) in tumors. Antiproliferative and proapoptotic effects of silibinin were associated with down-regulation of extracellular signal-regulated kinase 1/2 (ERK1/2) and Akt phosphorylation as well as cyclin D1 expression. Antiangiogenic effect of silibinin was coupled with a strong decrease in inducible nitric oxide synthase (NOS) and NOS3, cyclooxygenase-1 (COX-1) and COX-2, and hypoxia-inducing factor-1α (HIF-1α) and vascular endothelial growth factor (VEGF). These findings suggest *in vivo* antitumor efficacy of silibinin against CRC involving its antiproliferative, proapoptotic, and antiangiogenic activities. The inhibition of ERK1/2 and Akt signaling may account for antiproliferative and proapoptotic effects, whereas down-regulation of NOS, COX, HIF-1α, and VEGF expression could lead to antiangiogenic effect of silibinin against CRC. Overall, potential use of silibinin against human CRC could be suggested. [Cancer Res 2008;68(6):2043–50]

Introduction

Colorectal cancer (CRC) is a major public health concern around the world and is the third most common cancer in the United States (1). Recent statistics suggest an estimated 153,760 new cases of CRC with 52,180 deaths in 2007 (1, 2). Although genetic defects, such as mutation in adenomatous polyposis coli and loss of tumor suppressor p53, are involved in initiation and progression of CRC, the epigenetic alterations controlling tumor cell proliferation, survival, inflammation, and angiogenesis also play critical roles in CRC growth and progression (3–8). In many instances, high cell proliferation activity, resistance to apoptosis, and enhanced tumor angiogenesis are associated with the poor prognosis of solid tumors, including CRC (7, 9, 10). An enhanced tumor cell proliferation activity is usually accompanied with aberrant cell cycle progression, and in this regard, CRC expresses high level of cyclin D1 (11). The use of nonsteroidal anti-inflammatory drugs exerts antitumor effects against CRC (8), where inflammation favors proliferation as well as angiogenesis that support the role of inflammatory mechanisms in growth and progression of CRC (12). Tumor angiogenesis has been observed as an essential component to support the growth of solid tumors beyond a critical size and provide a viable route for tumor metastasis to distant organs (10). Therefore, it has been hypothesized that chemopreventive agents that could overcome these epigenetic defects could be potentially effective in controlling CRC.

Our completed studies show that silibinin has both promise and potential to inhibit the growth of solid tumors, including skin, prostate, and lung, in animal models (13–15). Silibinin is nontoxic and has human acceptance as it is used clinically and consumed as dietary supplement for its hepatoprotective effect (16, 17). Although silymarin, the parent mixture of the pure and major biologically active compound silibinin, is shown to inhibit azoxymethane-induced colon carcinogenesis in male F344 rats (18), the underlying mechanisms of action remain to be elucidated. Further, until now, the pure compound silibinin has not been studied for its *in vivo* efficacy and mechanism against CRC, although our completed *in vitro* study with silibinin in human CRC HT29 cells has shown strong antiproliferative effect (19).

In the present study, we examined *in vivo* efficacy of oral silibinin as well as silybin-phytosome (it shows better bioavailability than pure silibinin) against human CRC HT29 tumor xenograft growth in athymic nude mice. Additional studies performed include analysis of extensively used biomarkers in preclinical cancer models, such as proliferation cell nuclear antigen (PCNA), apoptosis, and tumor microvessel density. We also identified potential molecular targets of silibinin, including extracellular signal-regulated kinase1/2 (ERK1/2) and protein kinase B (Akt) signaling, nitric oxide synthase (NOS), cyclooxygenase (COX), and hypoxia-inducing factor-1α (HIF-1α) and vascular endothelial growth factor (VEGF), for its antiproliferative, proapoptotic, and antiangiogenic effects against HT29 tumor growth.

Materials and Methods

Cell lines, animals, and chemicals. HT29 cell line was from the American Type Culture Collection and grown in DMEM (Technologies, Inc.) with 10% serum (Hyclone), 100 units/mL penicillin, and 100 μg/mL streptomycin under standard conditions. Six-week-old athymic BALB/c *nu/nu* male mice were from the National Cancer Institute (Frederick, MD). Animal care was in accordance with current regulations and standards of NIH and our institutional guidelines. Silibinin, carboxymethyl cellulose (CMC), and phosphatidylcholine (PC) were from Sigma-Aldrich Chemical

Requests for reprints: Rajesh Agarwal, Department of Pharmaceutical Sciences, University of Colorado Denver, 4200 East 9th Street, Box C238, Denver, CO 80262. Phone: 303-315-1381; Fax: 303-315-6281; E-mail: Rajesh.Agarwal@uchsc.edu.

doi:10.1158/0008-5472.CAN-07-6247

Co. Silybin-phytosome that contains silibinin and PC in 1:2 ratio for better bioavailability of silibinin was obtained from Indena.

***In vivo* tumor xenograft study.** HT29 cells were grown in culture and then detached by trypsinization, washed, and resuspended in serum-free DMEM. Six-week-old athymic BALB/c *nu/nu* male mice were given a s.c. injection of 4×10^6 HT29 cells mixed with Matrigel (1:1) in the right flank to initiate tumor growth. After 5 days of xenograft implantation when tumor sizes reached ~3 mm in diameter, mice were randomly divided into five groups and gavaged with the following: (*a*) control group ($n = 8$), 0.5% (w/v) CMC (vehicle); (*b*) SB-200 ($n = 9$), 200 mg/kg/d dose of silibinin in CMC; (*c*) SP-100 ($n = 9$), 300 mg/kg/d dose of silybin-phytosome in CMC; (*d*) SP-200 ($n = 9$), 600 mg/kg/d dose of silybin-phytosome in CMC; and (*e*) PC ($n = 9$), 400 mg/kg/d dose of PC in CMC. All treatments were given 5 days a week for 32 days. Body weight and diet consumption were recorded twice weekly throughout the study. Tumor sizes were measured twice weekly and volume was calculated as reported recently (14). At the end of experiment, tumors were excised and weighed, and part of tumor was fixed in buffered formalin and the remaining was stored at −80°C. Based on tumor data, only tumor samples from control and SB-200 groups were processed for biomarker and molecular analysis.

Immunohistochemical staining for PCNA, cyclin D1, CD31, VEGF, inducible NOS, COX-2, and HIF-1α in tumors. Tumor samples fixed in 10% buffered formalin for 12 h were processed conventionally for paraffin-embedded tumor sections (5 μm thick). Sections were subjected to antigen retrieval and blocking of endogenous peroxidase activity (15). For immunostaining, sections were incubated with mouse monoclonal anti-PCNA (1:250 dilution; Dako), rabbit polyclonal anti–cyclin D1 (1:100 dilution; Santa Cruz Biotechnology, Inc.), goat polyclonal anti-CD31 (1.200 dilution; Santa Cruz Biotechnology), rabbit polyclonal anti-VEGF (1:100 dilution; Santa Cruz Biotechnology), rabbit polyclonal anti–inducible NOS (iNOS; 1:100 dilution; BD Transduction Laboratories), rabbit polyclonal anti-COX-2 (1:50 dilution; Santa Cruz Biotechnology), or rabbit polyclonal anti–HIF-1α (1:100 dilution; Novus Biologicals, Inc.) antibody. Sections were then incubated with biotinylated appropriate secondary antibody followed by conjugated horseradish peroxidase (HRP)-streptavidin (Dako) followed by incubation with 3,3′-diaminobenzidine (DAB; Sigma) working solution at room temperature and counterstaining with diluted Harris hematoxylin (Sigma). In all immunohistochemical staining, to rule out any nonspecific staining, negative staining controls were used, where, as required, sections were incubated with N-Universal Negative Control mouse or rabbit antibody (Dako) under identical conditions.

Quantification of immunostaining in tumors. Proliferating cells were quantified by counting PCNA-positive cells and total number of cells at five arbitrarily selected fields from each tumor at ×400 magnification. Proliferation index was determined as number of PCNA-positive cells × 100 / total number of cells (15). Endothelial cells (microvessels) were quantified by counting CD31-positive cells at five arbitrarily selected fields from each tumor at ×400 magnification. Microvessel density was determined as number of CD31-positive cells/×400 microscopic field (15). VEGF, iNOS, and COX-2 were quantified by counting respective positive cells and total number of cells at 10 randomly selected fields from each tumor at ×400 magnification, and data are presented as percent positive cells. HIF-1α immunoreactivity in tumors was mostly localized to the nucleus, which correlates with its transcriptional activity. Therefore, we quantified HIF-1α–positive nuclei at 10 randomly selected fields from each tumor at ×400 magnification as well as total number of nuclei, and the data are presented as percent HIF-1α–positive nuclei.

***In situ* apoptosis detection by terminal deoxynucleotidyl transferase–mediated dUTP nick end labeling staining.** The 5-μm-thick sections of tumor samples (those used for PCNA staining) were analyzed by terminal deoxynucleotidyl transferase (TdT)-mediated dUTP nick end labeling (TUNEL) staining using TumorTACS *In situ* Apoptosis kit (R&D Systems, Inc.) as published recently (14). Apoptotic cells were counted as DAB-positive cells (brown stained) at five arbitrarily selected microscopic fields at ×400 magnification, together with total number of cells, and apoptotic index was calculated as number of apoptotic cells × 100 / total number of cells (14).

Preparation of tumor homogenate and Western immunoblotting. Randomly, three tumors were selected each from control and SB-200 groups and homogenized in nondenaturing lysis buffer using Polytron and centrifuged at 14,000 × *g* followed by protein concentration determination in supernatants as reported earlier (15). Equal protein per lysate was resolved on Tris-glycine gel, transferred onto nitrocellulose membrane, and blocked for 1 h with 5% nonfat dry milk. Membranes were incubated with desired primary antibody overnight at 4°C and then with appropriate HRP-conjugated secondary antibody followed by enhanced chemiluminescence detection. Blots were scanned with Adobe Photoshop 6.0 with minimum background. Membranes were stripped and reprobed with anti–β-actin antibody for loading control.

Statistical and microscopic analyses. Statistical analysis was done with SigmaStat software version 2.03 (Jandel Scientific). Quantitative data are presented as mean and SE. Microscopic immunohistochemical analysis was done by Zeiss Axioskop 2 microscope (Carl Zeiss, Inc.) and photomicrographs were captured by Carl Zeiss AxioCam MRc5 camera. Statistical significance of difference between control and silibinin-fed group was determined by Student's *t* test and $P < 0.05$ was considered significant.

Results

Silibinin feeding inhibits HT29 tumor xenograft growth in nude mice. To study silibinin efficacy on CRC development, its gavage feeding was started to nude mice at day 6 after the xenograft implantation, a time at which HT29 xenografts were visibly and measurably established (~3 mm in diameter). We used two forms of silibinin in CMC vehicle: (*a*) pure silibinin and (*b*) silybin-phytosome; the latter is known for its better absorption in the gut. Progressive tumor growth was observed in control groups of mice on CMC or PC in CMC during the experiment (data not shown); however, the latter one showed a slightly lower tumor volume and weight, although statistically insignificant (Fig. 1*A* and *B*). Compared with control (CMC), silibinin treatment by oral gavage at 200 mg/kg/d dose, 5 days a week for 32 days, showed suppression of tumor xenograft growth throughout the study (data not shown). At the end, tumor volume per mouse was 933 ± 141 mm^3 in silibinin (SB-200) treatment group compared with $1{,}787 \pm 173$ mm^3 ($P = 0.002$) in control, accounting for a 48% decrease in tumor volume (Fig. 1*A*). Consistent with this observation, silibinin caused 42% decrease in tumor weight ($P = 0.012$) compared with control (0.74 ± 0.08 g/mouse in silibinin-treated group versus 1.28 ± 0.18 g/mouse in control; Fig. 1*B*). Compared with silibinin, silybin-phytosome showed greater antitumor efficacy. The lower dose of silybin-phytosome (100 mg/kg) showed almost equivalent effect to that of 200 mg/kg dose of silibinin in decreasing tumor volume and weight (Fig. 1*A* and *B*), and higher dose of silybin-phytosome showed better antitumor effect compared with its lower dose (Fig. 1*A* and *B*).

We also monitored whether silibinin or silybin-phytosome feeding causes any adverse health effect during the study by measuring body weight gain and diet consumption profiles, which are relevant and widely used primary indicators to assess gross toxicity of a test compound in intervention studies. Oral treatment of both silibinin and silybin-phytosome did not affect body weight gain and diet consumption profiles, which were almost comparable with their respective control groups (Fig. 1*C* and *D*). Together, these findings suggested an *in vivo* antitumor efficacy of silibinin against human CRC tumor xenograft in nude mice without any apparent signs of toxicity. Based on comparable observations, for biomarkers and molecular analyses, we used tumor samples only from control and pure silibinin-treated (SB-200) groups.

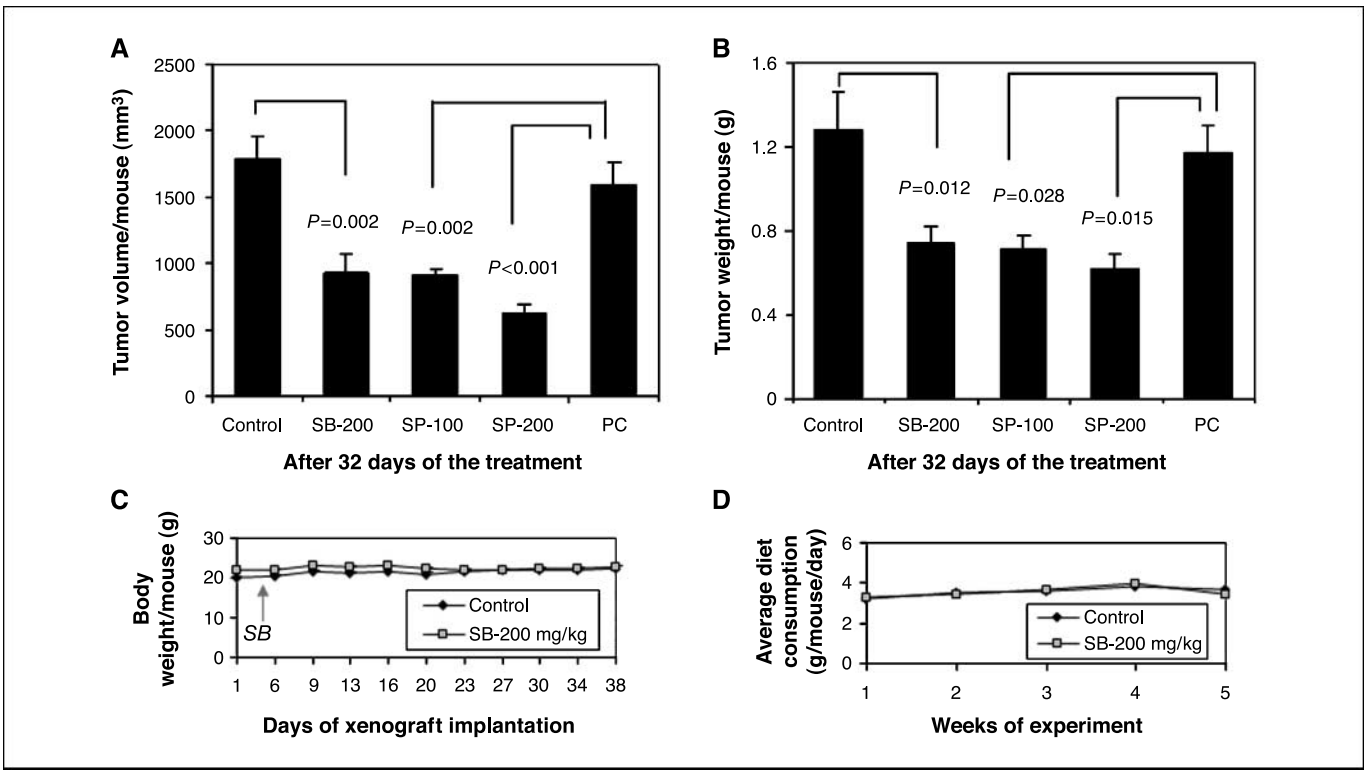

Figure 1. Effect of oral silibinin feeding on HT29 colorectal tumor xenograft growth, and body weight gain and diet consumption profiles in athymic nude mice. Four million HT29 cells were s.c. injected in the right flank of each mouse to initiate ectopic tumor growth. CMC or silibinin (200 mg/kg/d silibinin or 300 and 600 mg/kg/d silybin-phytosome in CMC, 5 d/wk) feeding by gavage started after 6 d of tumor cell injection and continued for 32 d. Similarly, PC (400 mg/kg) was given in CMC as control for silybin-phytosome that constitutes two-third PC. Final tumor volume (mm^3) per mouse (*A*) and tumor weight (g) per mouse (*B*) at the end of study. Body weight per mouse (*C*) and average diet consumption per mouse per day (*D*) were noted as a function of time. *A* and *B, columns,* mean of eight to nine samples from individual mouse in each group; *bars,* SE. *SB-200,* 200 mg/kg silibinin; *SP-100,* 300 mg/kg silybin-phytosome; *SP-200,* 600 mg/kg silybin-phytosome.

Silibinin inhibits tumor cell proliferation and induces apoptosis. The *in vivo* antiproliferative and apoptotic responses of silibinin causing inhibition of CRC xenograft growth were assessed by analyzing tumor samples for PCNA and TUNEL immunostaining. Qualitative microscopic assessment of PCNA-stained tumor sections showed a considerable decrease in PCNA immunoreactivity in silibinin-treated group compared with control (data not shown). The quantification of PCNA-positive cells in tumors showed that silibinin (200 mg/kg dose) treatment to nude mice results in 40% ($P < 0.001$) decrease in proliferation index compared with control (21 $\pm$ 4% PCNA-positive cells in silibinin versus 35 $\pm$ 3% in control group; Fig. 2*A*). The negative controls, where control IgG was used instead of anti-PCNA antibody, did not show any considerable positive staining (data not shown). The antiproliferative effect of silibinin was further confirmed by immunoblot analysis where tumor samples from silibinin-treated group showed a marked decrease in PCNA protein expression compared with controls (Fig. 2*B*).

Tumor sections examined for apoptotic cells showed an increased number of TUNEL-positive brown cells in silibinin-treated group compared with control (data not shown). The quantification of apoptosis showed that silibinin (200 mg/kg dose) increases apoptotic index by ~2-fold ($P < 0.001$) in tumors over that of control (Fig. 2*C*); however, this effect could be relatively less significant (as only 1% apoptotic cells were observed in silibinin-treated tumors) when compared with antiproliferative effect of silibinin in terms of its role in inhibiting tumor growth. Staining procedure was verified by using TACS-nuclease as positive control, which generated DNA fragments and showed positive staining in all nuclei, whereas labeling buffer was used instead of TdT in negative control that did not show any positive staining (data not shown). Overall, these results suggested a predominating role of *in vivo* antiproliferative effect of silibinin in suppressing HT29 tumor xenograft growth.

Silibinin decreases cyclin D1 expression in tumors. Cyclin D1 is overexpressed in rapidly cycling cells that propel G_1-S phase transition and correlates with enhanced proliferation (11). Because PCNA analysis showed antiproliferative effect of silibinin, we also analyzed its effect on cyclin D1 expression in tumors, where microscopic analysis of cyclin D1–stained tumors showed lesser immunoreactivity in silibinin-treated group compared with controls (Fig. 2*D, left*). The quantification of cyclin D1–positive cells showed 38 $\pm$ 1% cells in control versus 17 $\pm$ 1% cells (55% decrease; $P = 0.005$) in silibinin-treated group (Fig. 2*D, right*). Further, we confirmed this finding by immunoblot analysis of tumor lysate in which silibinin-treated group showed lower cyclin D1 protein expression compared with control (Fig. 2*B*). These results suggested that silibinin could inhibit *in vivo* cell cycle progression through G_1-S transition in HT29 tumors as one of its potential antiproliferative mechanisms.

Silibinin inhibits ERK1/2 and Akt activation in tumors. Activation of ERK1/2 and Akt signaling is involved in the growth and progression of many types of solid tumors, including CRC (7, 20). Targeting these signaling pathways has shown inhibition of

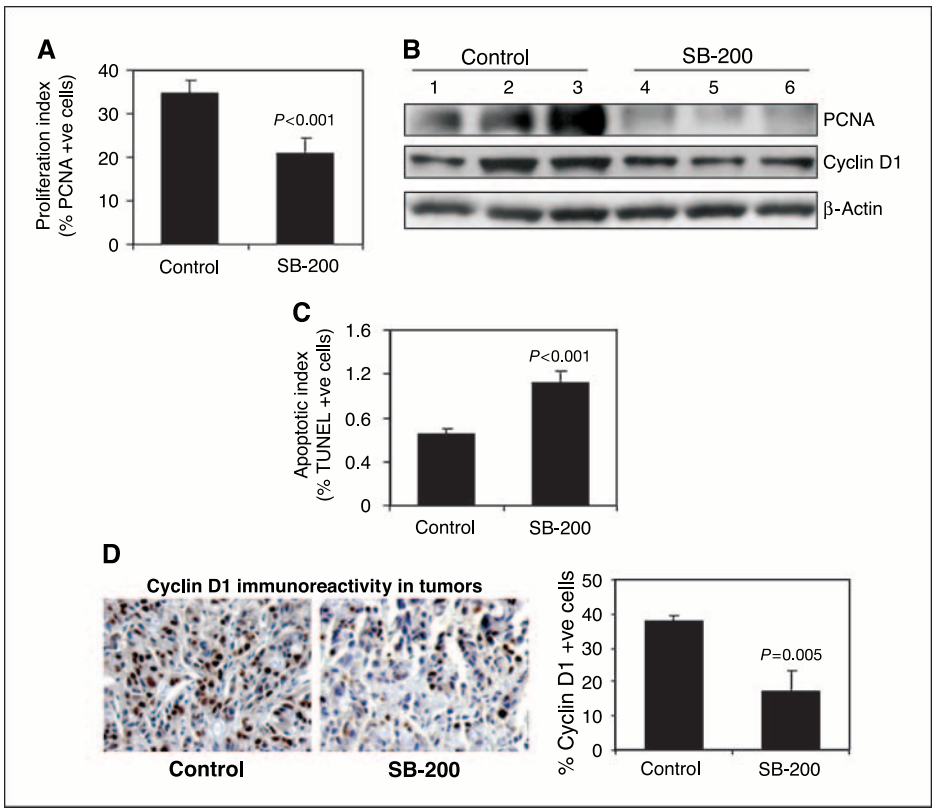

Figure 2. *In vivo* antiproliferative and proapoptotic effects of silibinin in human CRC HT29 tumor xenograft in nude mice. At the end of the study detailed in Fig. 1, a portion of each tumor from control and silibinin-treated (*SB-200*) groups was processed for immunohistochemical staining for PCNA, TUNEL, and cyclin D1 as described in Materials and Methods. Quantitative data for proliferation and apoptotic indices are shown as percent PCNA-positive cells (*A*) and percent TUNEL-positive cells (*C*), respectively. *D,* representative immunohistochemical data for cyclin D1 immunoreactivity (×400 magnification) and its quantification as percent cyclin D1–positive cells. *Columns,* mean of eight to nine samples from individual mouse in each group; *bars,* SE. *B,* a portion of three randomly selected tumors from each group were homogenized for lysate preparation and analyzed by Western blot analysis for PCNA and cyclin D1 expression as detailed in Materials and Methods. Membrane was stripped and reprobed for β-actin as a loading control.

tumor growth and progression in many studies (7). Because we observed that silibinin strongly decreases cell proliferation with slight increase in apoptosis, its effect on the activation of both ERK1/2 and Akt was next examined in HT29 tumors. Western blot analysis of randomly selected tumor samples showed relatively lower levels of phosphorylated ERK1/2 and phosphorylated Akt in silibinin-treated group compared with control without any considerable change in their total protein levels and β-actin was used as a loading control (Fig. 3). These results suggested that *in vivo* antiproliferative and proapoptotic activity of silibinin in HT29 tumors could be mediated by the down-regulation of ERK1/2 and Akt signaling.

Silibinin inhibits tumor microvessel density and VEGF expression. Tumor microvessel density is considered as a vital prognostic biomarker correlating with growth and development of CRC (21). To assess whether silibinin-caused inhibition of HT29 tumor growth is accompanied by its *in vivo* antiangiogenic effect, we examined intratumoral microvessel density by immunohistochemical analysis of CD31 endothelial cell–specific marker. Microscopic examination of tumors showed numerous CD31-stained cells in control group but only few in silibinin-treated group (data not shown). The quantification of CD31-positive cells in tumors showed 38 ± 8 CD31-positive cells/×400 field in control compared with 24 ± 5 in silibinin-treated group, accounting for 37% decrease ($P < 0.001$) in tumor microvessel density by silibinin (Fig. 4*A*). This observation suggests that inhibition of tumor angiogenesis by silibinin could have contributed to the inhibition of HT29 tumor growth in mice, which was next supported by VEGF analysis.

VEGF is the most critical molecular player for angiogenesis (22), and therefore, we also examined silibinin effect on VEGF expression in HT29 tumors. Immunostaining for VEGF revealed lower immunoreactivity in tumors from the silibinin-treated group of mice (Fig. 4*B*), and the quantification showed 42 ± 1% and 20 ± 1% VEGF-positive cells in control and silibinin-treated groups, respectively (Fig. 4*C*). This accounted for a 52% ($P < 0.001$) decrease in VEGF-positive cells by silibinin. We further confirmed the effect of silibinin on VEGF level by immunoblotting of randomly selected tumors from both groups. A strong decrease in VEGF protein level was observed in the tumor samples from silibinin group compared with control without considerable variation in β-actin as a protein loading control (Fig. 4*D*).

Silibinin decreases NOS expression in tumors. Up-regulation of NOS, specifically iNOS and NOS3 (endothelial NOS), induces many physiologic processes, including angiogenesis (23, 24). Consistently, we observed strong immunoreactivity for iNOS in HT29 tumors, which decreased substantially in silibinin-treated tumors (Fig. 5*A, left*). The quantification of iNOS immunostaining showed 46 ± 2% iNOS-positive cells in control compared with 14 ± 1% in silibinin-treated group, accounting for 70% decrease ($P < 0.001$) in iNOS-positive cells (Fig. 5*A, right*). To further support these findings, immunoblot analysis was next performed that also showed a strong decrease in iNOS protein level in silibinin-treated tumors (Fig. 6*A*). We also analyzed the expression of other two NOS family members, NOS1 (neuronal NOS) and NOS3, in both control and silibinin-treated tumors. Silibinin did not show any effect on NOS1 but strongly decreased the protein level of NOS3, which is associated with endothelial cells (Fig. 6*A*), without considerable change in β-actin as a protein loading control (Fig. 6*A*). These results indicate that tumor-associated iNOS and NOS3, which regulate tumor angiogenesis, could be potential molecular targets for the antitumor effect of silibinin.

Silibinin decreases COX expression in tumors. COX-2 has been strongly implicated in angiogenesis as well as in intestinal and

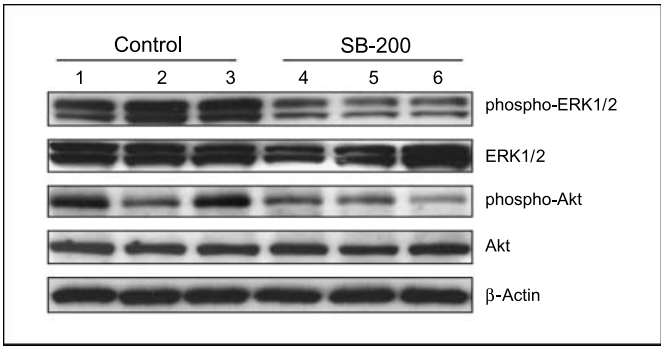

Figure 3. Effect of oral silibinin on ERK1/2 and Akt activation in HT29 tumors. Three randomly selected tumors from individual mouse in each group were analyzed by Western blot for phosphorylated and total levels of ERK1/2 and Akt by using specific antibodies as detailed in Materials and Methods. Membrane was stripped and reprobed for β-actin as a loading control. *SB-200,* 200 mg/kg silibinin for 5 d/wk.

colon tumor growth (25). Accordingly, silibinin effect on COX-2 expression was next examined by immunohistochemistry in tumors where control group samples showed marked immunoreactivity for COX-2 that decreased substantially in the tumors from silibinin-treated mice (Fig. 5*B, left*). Quantification of COX-2 staining in tumors showed 45 ± 2% COX-2–positive cells in control versus 22 ± 1% in silibinin-treated group, accounting for 51% ($P < 0.001$) decrease from that of control (Fig. 5*B, right*). These results were further confirmed by immunoblot analysis, which also showed high level of COX-2 protein in control tumor samples and a strong decrease by silibinin treatment (Fig. 6*B*); COX-1 protein expression was also decreased in silibinin-treated tumors (Fig. 6*B*), without considerable change in β-actin as a protein loading control (Fig. 6*B*). These results indicate that, in addition to iNOS and NOS3, silibinin could also target tumor-associated COX-1 and COX-2 expression for its antitumor and antiangiogenic effects.

Silibinin decreases HIF-1α expression in tumors. HIF-1α is overexpressed in angiogenic tumors and during low oxygen tension in tissues to initiate angiogenesis and has been implicated in solid tumor growth, including colon cancer (26, 27). Because antiangiogenic effect of silibinin was observed in HT29 tumors, we further examined whether silibinin has any effect on HIF-1α expression. In immunohistochemical analysis, tumors from control group showed clear immunoreactivity for HIF-1α, and importantly, it was localized within the nucleus, representing the transcriptionally active form of HIF-1α (Fig. 5*C, left*). However, the nuclear immunoreactivity of HIF-1α was considerably decreased in tumors from silibinin-treated mice (Fig. 5*C, left*). Quantification of nuclear HIF-1α immunostaining in tumors showed 20 ± 1% HIF-1α–positive nuclei in control versus 13 ± 1% in silibinin-treated mice (Fig. 5*C, right*), which accounted for a 35% ($P < 0.001$) decrease in HIF-1α–positive nuclei in HT29 tumors by silibinin. These results were further confirmed by immunoblot analysis, which also showed high level of HIF-1α protein in control tumor samples and a strong decrease by silibinin treatment (Fig. 6*B*), without considerable change in β-actin as a protein loading control (Fig. 6*B*). These results indicate that, in addition to iNOS, NOS3, COX-1, and COX-2, silibinin could also target tumor-associated expression of HIF-1α for its antiangiogenic effect.

Discussion

The central findings in the present study are that (*a*) oral silibinin feeding suppresses the growth of human CRC HT29 tumor xenografts in athymic nude mice without any noticeable toxicity; (*b*) silybin-phytosome (a formulation for enhanced absorption of silibinin) shows greater antitumor efficacy compared with pure silibinin; and (*c*) antitumor effect of silibinin was associated with a decrease in proliferation index as observed by reduced PCNA and cyclin D1 expression, a slight increase in apoptosis, and a strong inhibition of tumor angiogenesis as observed by CD31 and VEGF analyses. At molecular level, silibinin showed down-regulation of mitogenic and survival signaling as it decreased ERK1/2 and Akt phosphorylation in tumors. Silibinin also decreased the expression of iNOS, NOS3, COX-1, COX-2, and HIF-1α, which could be responsible for its strong antiangiogenic effect. These findings

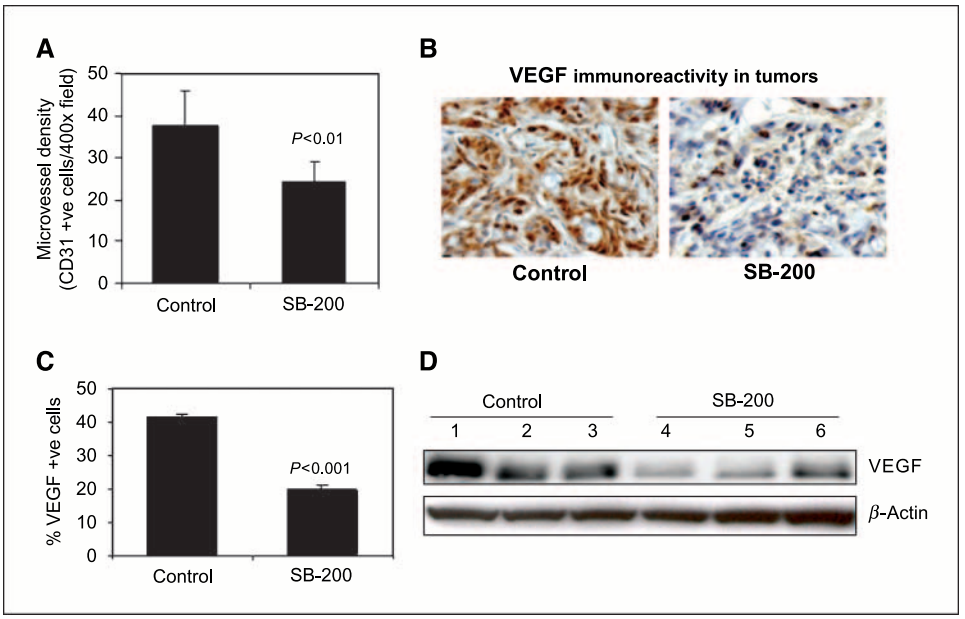

Figure 4. Effect of oral silibinin on HT29 tumor microvessel density and VEGF expression. *A,* at the end of the study detailed in Fig. 1, a portion of each tumor from control and silibinin-treated (*SB-200*) groups was processed for immunohistochemical staining for CD31 as described in Materials and Methods. Quantitative data for tumor endothelial cells are shown as number of CD31-positive endothelial cells per ×400 microscopic field. Representative immunohistochemical data for VEGF immunoreactivity (×400 magnification; *B*) and its quantification as percent VEGF-positive cells (*C*). *Columns,* mean of eight to nine samples from individual mouse in each group; *bars,* SE. *D,* a portion of three randomly selected tumors from each group were homogenized for lysate preparation and analyzed by Western blot analysis for VEGF expression as detailed in Materials and Methods. Membrane was stripped and reprobed for β-actin as a loading control. *SB-200,* 200 mg/kg silibinin for 5 d/wk.

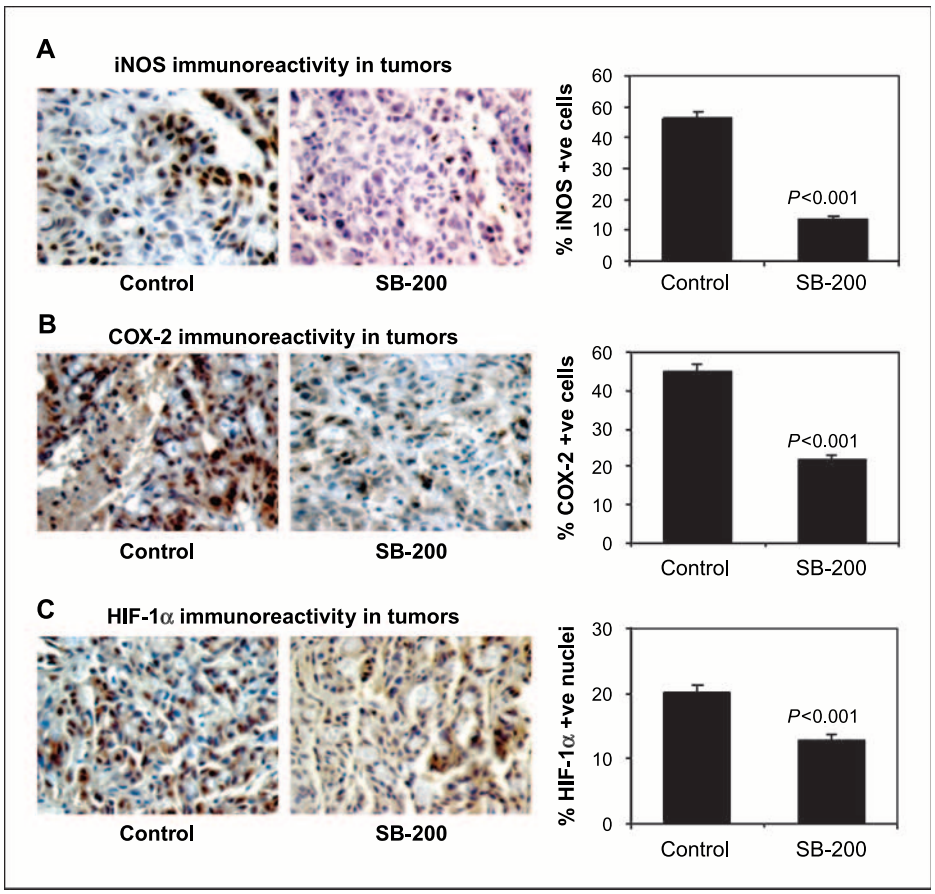

Figure 5. Effect of oral silibinin on iNOS, COX-2, and HIF-1α expression in HT29 tumors. At the end of the study detailed in Fig. 1, a portion of each tumor from control and silibinin-treated (*SB-200*) groups was processed for immunohistochemical staining for iNOS, COX-2, and HIF-1α as described in Materials and Methods. *A* to *C,* representative immunohistochemical data for immunoreactivity of these molecules are shown at ×400 magnification. The quantification of iNOS and COX-2 (*A* and *B*) was done as percent-positive (*brown*) cells, whereas for HIF-1α (*C*) it was done as percent-positive (*brown*) nuclei as detailed in Materials and Methods. *Columns,* mean of eight to nine samples from individual mouse in each group; *bars,* SE.

suggest further investigation of silibinin efficacy in other CRC animal models such as chemically induced and transgenic. Nevertheless, the findings in the present study support the promising usefulness of silibinin in CRC patients.

The solid tumor growth and progression essentially require unchecked cell proliferation, loss of apoptosis, and induction of angiogenesis, and these critical events are positively supported by growth factor receptor signaling, which becomes constitutively active in advanced stages of CRC (7, 20, 28). Indeed, several studies have shown the presence of multiple constitutively active mitogenic, cell survival, and antiapoptotic pathways in CRC, implying that targeting a single event may not be enough to accomplish the growth control of CRC. Consequently, it is likely that anticancer agents targeting multiple tumorigenic events, such as simultaneous inhibition of both mitogenic and cell survival signaling pathways as well as tumor angiogenesis, could be more effective in suppressing CRC growth and progression (28, 29). Consistent with this notion, in the present study, silibinin showed antitumor efficacy against human CRC tumor growth in nude mice involving diverse molecular alterations associated with cell proliferation, survival, and angiogenesis.

For the first time in this study, we also compared the antitumor efficacy of oral silybin-phytosome with pure silibinin in which silybin-phytosome showed comparatively greater efficacy than pure silibinin without any toxicity. Therefore, it was anticipated that, compared with silibinin, similar oral dose of silybin-phytosome will lead to the higher physiologic level of silibinin in mice. Indeed, this was the case as observed by silibinin estimation in mouse plasma (data not shown). The tumor growth inhibition by silibinin was accompanied by a decrease in proliferation index and a slight increase in apoptosis. A corresponding decrease in PCNA-positive and cyclin D1–positive cells as well as their protein expression by silibinin was also observed. Cyclin D1 has critical role in cell cycle progression from G_1 to S phase transition, whereas PCNA is a cofactor for DNA polymerase required for DNA synthesis during S phase (30, 31). Therefore, it is anticipated that silibinin-caused inhibition of tumor cell proliferation could be associated with G_1 phase arrest during cell cycle progression. This indeed is supported by our *in vitro* study where silibinin induced a strong G_1 arrest in HT29 cells (19). The *in vivo* apoptotic effect of silibinin on tumor cells was statistically significant, but it may not have major contribution in lowering the tumor growth because the number of apoptotic cells was very few, accounting for about only 1%.

The antiproliferative and proapoptotic effects of silibinin could be attributed to the inhibition of constitutively active mitogenic and cell survival signaling in colorectal tumors. As anticipated, silibinin decreased the phosphorylated levels of both ERK1/2 and Akt without any effect on their total protein levels in tumors. This observation indicated a specific effect causing down-regulation of signaling mediated through ERK1/2 and Akt that was more related to the antiproliferative effect of silibinin. ERK1/2 and Akt are conversing points for many mitogenic events initiated at membrane receptor or cytoplasmic levels (7, 20). PCNA is a downstream target of these signaling pathways that critically regulate cell proliferation (31). In this regard, in addition to the inhibition of ERK1/2 and Akt

signaling, silibinin also decreased PCNA-positive tumor cells, providing an *in vivo* molecular evidence for its antiproliferative activity and associated mechanisms.

Tumors can stay dormant for years due to a balance between cell proliferation and apoptosis in the absence of angiogenesis (21). In such condition, there is also a balance between proangiogenic and antiangiogenic factors (21). Tumor angiogenesis is facilitated by a shift in the equilibrium toward the proangiogenic environment. Therefore, levels of angiogenic inhibitors exceeding that of stimulators could inhibit tumor growth and progression. In this regard, many preclinical studies suggest that antiangiogenic strategy could be a promising approach for cancer control, which is less likely to acquire drug resistance (32–34). The quantification of tumor angiogenesis could be a measure of tumor staging for growth, invasive, and metastatic potential as well as for diagnosis (35). Consistent with antiangiogenic strategy, silibinin strongly inhibited the vascularization of CRC tumors as examined by immunohistochemical staining for endothelial cell–specific CD31 marker.

Solid tumors overexpress angiogenic factors, including VEGF, to recruit blood vessel for neoangiogenesis as well as to maintain vascular state of the tumor for its perpetual growth. VEGF is the most potent angiogenic factor for tumor angiogenesis, as intervention by inhibiting the production of VEGF or neutralizing the concentration of VEGF or blocking its receptor signaling has been shown to inhibit tumor growth (32–34). Many chemopreventive agents down-regulate VEGF production in imparting their antiangiogenic potential (29, 36, 37). In this study, silibinin also strongly decreased the level of VEGF expression in HT29 tumors. The decrease in tumor-associated VEGF by silibinin could be one of the important mechanisms in controlling angiogenesis and causing an inhibition of overall tumor growth. The effect of silibinin on VEGF was confirmed by both immunohistochemical and immunoblot analyses of tumors for VEGF expression. Together, our findings suggested that antiangiogenic potential of silibinin could be explored for lowering the risk of and preventing the growth and progression of CRC.

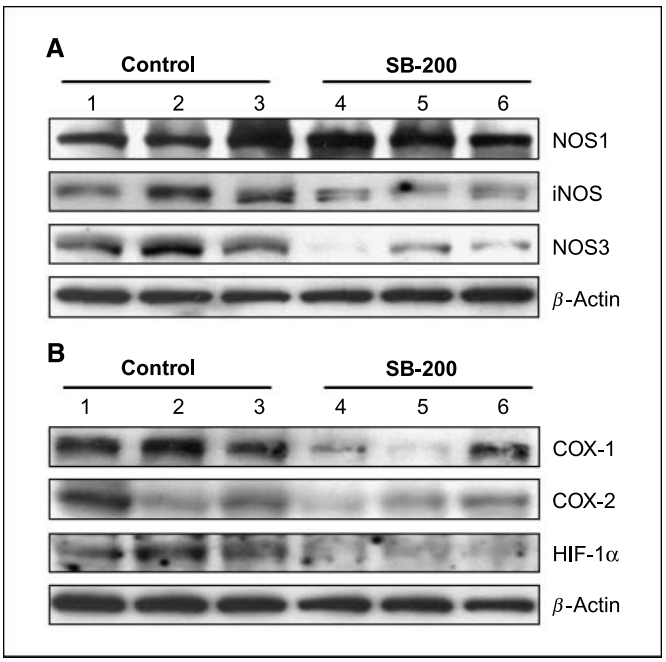

Figure 6. Effect of oral silibinin on NOS, COX, and HIF-1α expression in HT29 tumors. *A* and *B,* three randomly selected tumors from individual mouse in each group were analyzed by Western blot for levels of NOS1, NOS2, NOS3, COX-1, COX-2, and HIF-1α by using specific antibodies as detailed in Materials and Methods. Membranes were stripped and reprobed for β-actin as a loading control. *SB-200,* 200 mg/kg silibinin for 5 d/wk.

iNOS and NOS3 produce biological nitric oxide that plays an important role in favoring tumor angiogenesis that supports tumor growth and progression (38–41). iNOS is usually induced during pathologic conditions, whereas NOS3 is specifically produced by endothelial cells to support blood capillary formation (38). VEGF is also known to produce nitric oxide formation during angiogenesis (42). In the present study, high expression of both iNOS and NOS3 was observed in HT29 tumors in control group, which also showed high microvessel density, and silibinin treatment decreased the levels of both iNOS and NOS3 as well as tumor microvessel density. Similar to NOS, COX-2, a key enzyme for the synthesis of prostaglandins, is also involved in tumor angiogenesis, growth, and progression (43, 44). Some studies also show a link between iNOS and COX-2 expression (43). We observed that silibinin reduces the levels of tumor-associated COX-1 and COX-2; however, we have previously observed that silibinin does not have any effect on COX-1 in normal tissue (45). HIF-1α plays a pivotal role in pathophysiologic angiogenesis via transcriptional activation of VEGF (46). Overexpression of HIF-1α along with VEGF occurs in many cancers, including CRC (27, 46, 47). In the present study, HIF-1α–mediated up-regulation of VEGF could have been targeted by silibinin in HT29 tumors, as silibinin strongly decreased the nuclear level of HIF-1α with a concomitant decrease in VEGF expression. Further, ERK1/2 and Akt signaling are also known to induce VEGF expression through HIF-1α (48), which was also down-regulated by silibinin. Together, these findings suggest that growing HT29 tumors have high levels of iNOS, NOS3, COX-1, COX-2, and HIF-1α that could effectively mediate tumor angiogenesis and growth. Therefore, targeting these molecules could result in a decrease in tumor angiogenesis and shrinkage or slower growth of tumor size as observed with silibinin treatment in the present study.

Collectively, present findings provide *in vivo* evidence for antiproliferative, apoptotic, and antiangiogenic effects of silibinin, which were associated with the inhibition of human CRC tumor xenograft growth without any toxicity in mice. Down-regulation of ERK1/2 and Akt signaling by silibinin could be potential *in vivo* mechanisms to inhibit CRC growth. Silibinin-caused decrease in iNOS, NOS3, COX-1, COX-2, and HIF-1α expression could reduce VEGF production in tumor and suppress tumor angiogenesis. These findings provide preclinical evidence for antitumor efficacy of oral silibinin against human CRC as well as associated potential mechanisms and justify its further investigation in other CRC preclinical models to widen its scope and consideration for its usefulness in human CRC patients, which could be supported by the fact that silibinin is already successfully tested in phase I trial (49), and is now in phase II trial, in prostate cancer patients.

Acknowledgments

Received 11/14/2007; revised 12/21/2007; accepted 12/29/2007.

Grant support: National Cancer Institute RO1 grant CA112304.

The costs of publication of this article were defrayed in part by the payment of page charges. This article must therefore be hereby marked *advertisement* in accordance with 18 U.S.C. Section 1734 solely to indicate this fact.

References

1. Arber N, Levin B. Chemoprevention of colorectal cancer: ready for routine use? Recent Results Cancer Res 2005;166:213–30.
2. Jemal A, Siegel R, Ward E, Murray T, Xu J, Thun MJ. Cancer statistics, 2007. CA Cancer J Clin 2007;57:43–66.
3. Rupnarain C, Dlamini Z, Naicker S, Bhoola K. Colon cancer: genomics and apoptotic events. Biol Chem 2004; 385:449–64.
4. Kinzler KW, Vogelstein B. Lessons from hereditary colorectal cancer. Cell 1996;87:159–70.
5. Rodrigues NR, Rowan A, Smith MEF, et al. p53 mutations in colorectal cancer. Proc Natl Acad Sci U S A 1990;87:7555–9.
6. Samowitz WS, Slattery ML. Missense mismatch repair gene alterations, microsatellite instability, and hereditary nonpolyposis colorectal cancer. J Clin Oncol 2002; 20:1203–8.
7. Sebolt-Leopold JS, Dudley DT, Herrera R, et al. Blockade of the MAP kinase pathway suppresses growth of colon tumors *in vivo*. Nat Med 1999;5:736–7.
8. Gupta RA, Dubois RN. Colorectal cancer prevention and treatment by inhibition of cyclooxygenase-2. Nat Rev Cancer 2001;1:11–21.
9. Igney FH, Krammer PH. Death and anti-death: tumour resistance to apoptosis. Nat Rev Cancer 2002;2:277–88.
10. Carmeliet P, Jain RK. Angiogenesis in cancer and other diseases. Nat Med 2000;407:249–57.
11. Schwartz GK, Shah MA. Targeting the cell cycle: a new approach to cancer therapy. J Clin Oncol 2005;23: 9408–21.
12. Dalgleish AG, O'Byrne K. Inflammation and cancer: the role of the immune response and angiogenesis. Cancer Treat Res 2006;130:1–38.
13. Gu M, Singh RP, Dhanalakshmi S, Agarwal C, Agarwal R. Silibinin inhibits inflammatory and angiogenic attributes in photocarcinogenesis in SKH-1 hairless mice. Cancer Res 2007;67:3483–91.
14. Singh RP, Dhanalakshmi S, Tyagi AK, Chan DCF, Agarwal C, Agarwal R. Dietary feeding of silibinin inhibits advance human prostate carcinoma growth in athymic nude mice, and increases plasma insulin-like growth factor-binding protein-3 levels. Cancer Res 2002; 62:3063–9.
15. Singh RP, Deep G, Chittezhath M, et al. Effect of silibinin on the growth and progression of primary lung tumors in mice. J Natl Cancer Inst 2006;98:846–55.
16. Saller R, Meier R, Brignoli R. The use of silymarin in the treatment of liver diseases. Drugs 2001;6:2035–63.
17. Wellington K, Jarwis B. Silymarin: a review of its clinical properties in the management of hepatic disorders. BioDrugs 2001;15:465–89.
18. Kohno H, Tanaka T, Kawabata K, et al. Silymarin, a naturally occurring polyphenolic antioxidant flavonoid, inhibits azoxymethane-induced colon carcinogenesis in male F344 rats. Int J Cancer 2002;101:461–8.
19. Agarwal C, Singh RP, Dhanalakshmi S, et al. Silibinin upregulates the expression of cyclin-dependent kinase inhibitors and causes cell cycle arrest and apoptosis in human colon carcinoma HT-29 cells. Oncogene 2003;22: 8271–82.
20. Michl P, Downward J. Mechanisms of disease: PI3K/AKT signaling in gastrointestinal cancers. Z Gastroenterol 2005;43:1133–9.
21. Kerbel RS. Tumor angiogenesis: past, present and the near future. Carcinogenesis 2000;21:505–15.
22. Leung DW, Cachianes G, Kuang WJ, Goeddel DV, Ferrara N. Vascular endothelial growth factor is a secreted angiogenic mitogen. Science 1989;246:1306–9.
23. Palmer RM, Ferrige AG, Moncada S. Nitric oxide release accounts for the biological activity of endothelium-derived relaxing factor. Nature 1987;327:524–6.
24. Garcia-Cardena G, Folkman J. Is there a role for nitric oxide in tumor angiogenesis? J Natl Cancer Inst 1998;90: 560–1.
25. Rodríguez-Moranta F, Castells A. Mechanisms of colon cancer prevention with and beyond COX-2 inhibition. Curr Top Med Chem 2005;5:505–16.
26. Ben-Shoshan M, Amir S, Dang DT, Dang LH, Weisman Y, Mabjeesh NJ. 1α,25-Dihydroxyvitamin D3 (Calcitriol) inhibits hypoxia-inducible factor-1/vascular endothelial growth factor pathway in human cancer cells. Mol Cancer Ther 2007;6:1433–9.
27. Giles RH, Lolkema MP, Snijckers CM, et al. Interplay between VHL/HIF1α and Wnt/β-catenin pathways during colorectal tumorigenesis. Oncogene 2006;25: 3065–70.
28. Misra S, Toole BP, Ghatak S. Hyaluronan constitutively regulates activation of multiple receptor tyrosine kinases in epithelial and carcinoma cells. J Biol Chem 2006;281:34936–41.
29. Singh RP, Agarwal R. Tumor angiogenesis: a potential target in cancer control by phytochemicals. Curr Cancer Drug Targets 2003;3:205–17.
30. Kouraklis G, Theocharis S, Vamvakas P, et al. Cyclin D1 and Rb protein expression and their correlation with prognosis in patients with colon cancer. World J Surg Oncol 2006;4:5.
31. Moldovan GL, Pfander B, Jentsch S. PCNA, the maestro of the replication fork. Cell 2007;129:665–79.
32. Kim KJ, Li B, Winer J, et al. Inhibition of vascular endothelial growth factor-induced angiogenesis suppresses tumor growth *in vivo*. Nature 1993;362:841–4.
33. Benjamin LE, Golijanin D, Itin A, Pode D, Keshet E. Selective ablation of immature blood vessels in established human tumors follows vascular endothelial growth factor withdrawal. J Clin Invest 1999;103:159–65.
34. Borgstrom P, Hillan KJ, Sriramarao P, Ferrera N. Complete inhibition of angiogenesis and growth factor neutralizing antibody: novel concepts of angiostatic therapy from intravital videomicroscopy. Cancer Res 1996;56:4032–9.
35. Diaz-Rubio E. Vascular endothelial growth factor inhibitors in colon cancer. Adv Exp Med Biol 2006;587: 251–75.
36. Singh RP, Sharma G, Dhanalakshmi S, Agarwal C, Agarwal R. Suppression of advanced human prostate tumor growth in athymic mice by silibinin feeding is associated with reduced cell proliferation, increased apoptosis, and inhibition of angiogenesis. Cancer Epidemiol Biomarkers Prev 2003;12:933–9.
37. Singh RP, Dhanalakshmi S, Agarwal C, Agarwal R. Silibinin strongly inhibits growth and survival of human endothelial cells via cell cycle arrest and downregulation of survivin, Akt and NF-κB: implications for angioprevention and antiangiogenic therapy. Oncogene 2005;24: 1188–202.
38. Singh RP, Agarwal R. Inducible nitric oxide synthase-vascular endothelial growth factor axis: a potential target to inhibit tumor angiogenesis by dietary agents. Curr Cancer Drug Targets 2007;7:475–83.
39. Rao CV. Nitric oxide signaling in colon cancer chemoprevention. Mutat Res 2004;555:107–19.
40. Morbidelli L, Donnini S, Ziche M. Role of nitric oxide in tumor angiogenesis. Cancer Treat Res 2004;117: 155–67.
41. Rao CV, Indranie C, Simi B, Manning PT, Connor JR, Reddy BS. Chemopreventive properties of a selective inducible nitric oxide synthase inhibitor in colon carcinogenesis, administered alone or in combination with celecoxib, a selective cyclooxygenase-2 inhibitor. Cancer Res 2002;62:165–70.
42. Bussolati B, Dunk C, Grohman M, Kontos CD, Mason J, Ahmed A. Vascular endothelial growth factor receptor-1 modulates vascular endothelial growth factor-mediated angiogenesis via nitric oxide. Am J Pathol 2001;159:993–1008.
43. Watanabe K, Kawamori T, Nakatsugi S, Wakabayashi K. COX-2 and iNOS, good targets for chemoprevention of colon cancer. Biofactors 2000;12:129–33.
44. Chell S, Kadi A, Williams AC, Paraskeva C. Mediators of PGE2 synthesis and signaling downstream of COX-2 represent potential targets for the prevention/treatment of colorectal cancer. Biochim Biophys Acta 2006;1766: 104–19.
45. Zhao J, Sharma Y, Agarwal R. Significant inhibition by the flavonoid antioxidant silymarin against 12-*O*-tetradecanoylphorbol 13-acetate-caused modulation of antioxidant and inflammatory enzymes, and cyclooxygenase 2 and interleukin-1α expression in SENCAR mouse epidermis: implications in the prevention of stage I tumor promotion. Mol Carcinog 1999;26:321–33.
46. Lopez-Lazaro M. Hypoxia-inducible factor 1 as a possible target for cancer chemoprevention. Cancer Epidemiol Biomarkers Prev 2006;15:2332–5.
47. Fukuda R, Kelly B, Semenza GL. Vascular endothelial growth factor gene expression in colon cancer cells exposed to prostaglandin E2 is mediated by hypoxia-inducible factor 1. Cancer Res 2003;63:2330–4.
48. Fukuda R, Hirota K, Fan F, Jung YD, Ellis LM, Semenza GL. Insulin-like growth factor 1 induces hypoxia-inducible factor 1-mediated vascular endothelial growth factor expression, which is dependent on MAP kinase and phosphatidylinositol 3-kinase signaling in colon cancer cells. J Biol Chem 2002;277:38205–11.
49. Flaig TW, Gustafson DL, Su LJ, et al. A phase I and pharmacokinetic study of silybin-phytosome in prostate cancer patients. Invest New Drugs 2007;25: 139–46.

Silibinin Inhibits Colorectal Cancer Growth by Inhibiting Tumor Cell Proliferation and Angiogenesis

Rana P. Singh, Mallikarjuna Gu and Rajesh Agarwal

Cancer Res 2008;68:2043-2050.